

Finding Planet Nine: apsidal anti-alignment Monte Carlo results

C. de la Fuente Marcos^{*} and R. de la Fuente Marcos

Apartado de Correos 3413, E-28080 Madrid, Spain

Accepted 2016 July 19. Received 2016 July 13; in original form 2016 March 29

ABSTRACT

The distribution of the orbital elements of the known extreme trans-Neptunian objects or ETNOs has been found to be statistically incompatible with that of an unperturbed asteroid population following heliocentric or, better, barycentric orbits. Such trends, if confirmed by future discoveries of ETNOs, strongly suggest that one or more massive perturbers could be located well beyond Pluto. Within the trans-Plutonian planets paradigm, the Planet Nine hypothesis has received much attention as a robust scenario to explain the observed clustering in physical space of the perihelia of seven ETNOs which also exhibit clustering in orbital pole position. Here, we revisit the subject of clustering in perihelia and poles of the known ETNOs using barycentric orbits, and study the visibility of the latest incarnation of the orbit of Planet Nine applying Monte Carlo techniques and focusing on the effects of the apsidal anti-alignment constraint. We provide visibility maps indicating the most likely location of this putative planet if it is near aphelion. We also show that the available data suggest that at least two massive perturbers are present beyond Pluto.

Key words: methods: statistical – celestial mechanics – minor planets, asteroids: general – Oort Cloud – planets and satellites: detection – planets and satellites: general.

1 INTRODUCTION

The distribution of the orbital parameters of the known extreme trans-Neptunian objects or ETNOs is statistically incompatible with that of an unperturbed asteroid population following Keplerian orbits (de la Fuente Marcos & de la Fuente Marcos 2014, 2016b; Trujillo & Sheppard 2014; de la Fuente Marcos, de la Fuente Marcos & Aarseth 2015, 2016; Gomes, Soares & Brasser 2015; Batygin & Brown 2016; Brown & Batygin 2016; Malhotra, Volk & Wang 2016). A number of plausible explanations have been suggested. These include the possible existence of one (Trujillo & Sheppard 2014; Gomes et al. 2015; Batygin & Brown 2016; Brown & Batygin 2016; Malhotra et al. 2016) or more (de la Fuente Marcos & de la Fuente Marcos 2014, 2016b; de la Fuente Marcos et al. 2015, 2016) trans-Plutonian planets, capture of ETNOs within the Sun’s natal open cluster (Jílková et al. 2015), stellar encounters (Brasser & Schwamb 2015; Feng & Bailer-Jones 2015), being a by-product of Neptune’s migration (Brown & Firth 2016) or the result of the inclination instability (Madigan & McCourt 2016), and having been induced by Milgromian dynamics (Paučo & Klačka 2016).

At present, most if not all of the unexpected orbital patterns found for the known ETNOs seem to be compatible with the trans-Plutonian planets paradigm that predicts the presence of one or more planetary bodies well beyond Pluto. Within this paradigm, the best studied theoretical framework is that of the so-called Planet Nine hypothesis, originally suggested by Batygin & Brown (2016) and further developed in Brown & Batygin (2016). The goal of

this analytically and numerically supported conjecture is not only to explain the observed clustering in physical space of the perihelia and the positions of the orbital poles of seven ETNOs (see Appendix A for further discussion), but also to account for other, previously puzzling, pieces of observational evidence like the existence of low perihelion objects moving in nearly perpendicular orbits. The Planet Nine hypothesis is compatible with existing data (Cowan, Holder & Kaib 2016; Fienga et al. 2016; Fortney et al. 2016; Ginzburg, Sari & Loeb 2016; Linder & Mordasini 2016) but, if Planet Nine exists, it cannot be too massive or bright to have escaped detection during the last two decades of surveys and astrometric studies (Luhman 2014; Cowan et al. 2016; Fienga et al. 2016; Fortney et al. 2016; Ginzburg et al. 2016; Linder & Mordasini 2016). A super-Earth in the sub-Neptunian mass range is most likely and such planet may have been scattered out of the region of the Jovian planets early in the history of the Solar system (Bromley & Kenyon 2016) or even captured from another planetary system (Li & Adams 2016; Mustill, Raymond & Davies 2016); super-Earths may also form at 125–750 au from the Sun (Kenyon & Bromley 2015, 2016).

The analysis of the visibility of Planet Nine presented in de la Fuente Marcos & de la Fuente Marcos (2016a) revealed probable locations of this putative planet based on data provided in Batygin & Brown (2016) and Fienga et al. (2016); the original data have been significantly updated in Brown & Batygin (2016). In addition, independent calculations (de la Fuente Marcos et al. 2016) show that the apsidal anti-alignment constraint originally discussed in Batygin & Brown (2016) plays a fundamental role on the dynamical impact of a putative Planet Nine on the orbital evolution

* E-mail: carlosdlfmarcos@gmail.com

Table 1. Pericentre distances, q , ecliptic coordinates at pericentre, (L_q, B_q) , and projected pole positions, (L_p, B_p) , of the 16 objects discussed in this paper computed using barycentric orbits, see also Figs 1 and 2. (Epoch: 2457600.5, 2016 July 31.0 00:00:00.0 TDB. J2000.0 ecliptic and equinox. Input data from the SBDB; data as of 2016 July 13.)

Object	q (au)	L_q ($^\circ$)	B_q ($^\circ$)	L_p ($^\circ$)	B_p ($^\circ$)
(82158) 2001 FP ₁₈₅	34.25	185.28	3.52	89.36	59.20
(90377) Sedna	76.19	96.31	-8.94	54.40	78.07
(148209) 2000 CR ₁₀₅	44.12	87.28	-15.39	38.29	67.24
(445473) 2010 VZ ₉₈	34.35	71.21	-3.26	27.40	85.49
2002 GB ₃₂	35.34	213.24	8.49	87.04	75.81
2003 HB ₅₇	38.10	208.32	2.88	107.87	74.50
2003 SS ₄₂₂	39.42	359.91	-8.28	61.05	73.21
2004 VN ₁₁₂	47.32	35.65	-13.59	336.02	64.45
2005 RH ₅₂	39.00	336.98	10.83	216.11	69.55
2007 TG ₄₂₂	35.56	39.41	-17.88	22.91	71.40
2007 VJ ₃₀₅	35.18	3.15	-4.40	294.38	78.02
2010 GB ₁₇₄	48.56	118.83	-4.65	40.71	68.44
2012 VP ₁₁₃	80.44	26.32	-21.94	0.80	65.95
2013 GP ₁₃₆	41.06	248.08	21.91	120.73	56.46
2013 RF ₉₈	36.28	27.88	-19.93	337.53	60.40
2015 SO ₂₀	33.17	28.89	-2.05	303.63	66.59

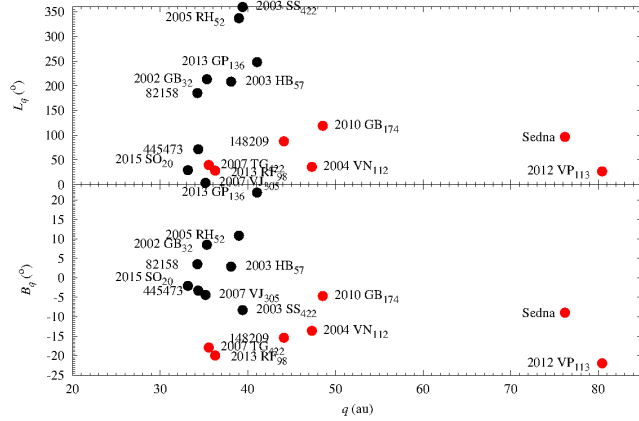


Figure 1. Pericentres of the objects in Table 1. The objects singled out in Brown & Batygin (2016) are plotted in red.

of the known ETNOs. Here, we improve the results presented in de la Fuente Marcos & de la Fuente Marcos (2016a) focusing on the effects of the apsidal anti-alignment constraint. This paper is organized as follows. Section 2 presents an analysis of clustering in barycentric elements, pericentre and orbital pole positions, which is subsequently discussed. An updated evaluation of the visibility of Planet Nine virtual orbits at aphelion is given in Section 3. Conclusions are summarized in Section 4.

2 CLUSTERING IN BARYCENTRIC PARAMETERS

The six (Batygin & Brown 2016) or seven (Brown & Batygin 2016) ETNOs singled out within the Planet Nine hypothesis (see Appendix A for details) have $a > 226$ au (heliocentric) and they exhibit clustering in perihelion location in absolute terms and also in orbital pole position. In order to better understand the context of these clusterings we study the line of apsides of the known ETNOs

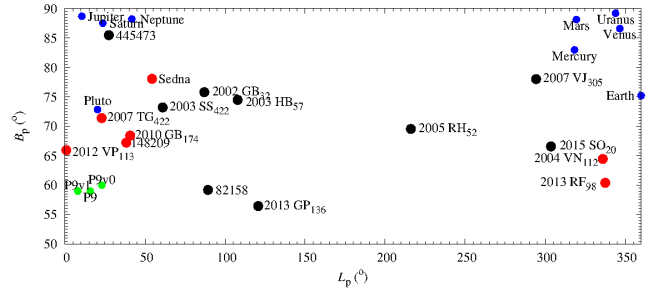


Figure 2. Poles of the objects in Table 1. Those singled out in Brown & Batygin (2016) are plotted in red, the known planets in blue, and various Planet Nine incarnations in green —P9v0 is the nominal solution in Batygin & Brown (2016), P9v1 is the one from Brown & Batygin (2016), and P9 is the previous one but enforcing apsidal anti-alignment.

(see Table 1 and Fig. 1) and the projection of their orbital poles on to the plane of the sky (see Table 1 and Fig. 2). Here, we consider barycentric orbits as it can be argued (see the discussion in Malhotra et al. 2016) that the use of barycentric orbital elements instead of the usual heliocentric ones is more correct in this case.

In Trujillo & Sheppard (2014), the ETNOs are defined as asteroids with heliocentric semimajor axis greater than 150 au and perihelion greater than 30 au; at present, there are 16 known ETNOs. Because of the nature of their orbits, the ETNOs cannot experience a close approach to the known planets, including Neptune. Nevertheless, the orbits of the ETNOs are affected by indirect perturbations that induce variations in perihelion location. The perihelion distance of an ETNO depends on the value of its semimajor axis and eccentricity, e , as it is given by $q = a(1 - e)$. However, its absolute position on the sky is only function of the inclination, i , the longitude of the ascending node, Ω , and the argument of perihelion, ω . In heliocentric ecliptic coordinates, the longitude and latitude of an object at perihelion, (l_q, b_q) , are given by the expressions: $\tan(l_q - \Omega) = \tan \omega \cos i$ and $\sin b_q = \sin \omega \sin i$ (see e.g. Murray & Dermott 1999). For an orbit with zero inclination, $l_q = \Omega + \omega$ and $b_q = 0^\circ$; therefore, if $i = 0^\circ$, the value of l_q coincides with that of the longitude of perihelion parameter, $\varpi = \Omega + \omega$. In Brown & Batygin (2016), l_q is called ‘perihelion longitude’ and b_q is the ‘perihelion latitude’. Considering barycentric orbits, we denote the barycentric ecliptic coordinates of an ETNO at pericentre as (L_q, B_q) . In Table 1 we show the values of q , L_q and B_q computed using the barycentric data in Table 2. The input values are from Jet Propulsion Laboratory’s Small-Body Database¹ (SBDB) and HORIZONS On-Line Ephemeris System (Giorgini et al. 1996).

Fig. 1 shows the position in the sky at pericentre as a function of the pericentre distance for the known ETNOs. The objects in Brown & Batygin (2016) are plotted in red; the average angular separation at pericentre for this group is $44^\circ \pm 30^\circ$, but the pair 2012 VP₁₁₃–2013 RF₉₈ has a separation of $2^\circ.5$, 2004 VN₁₁₂–2007 TG₄₂₂ has $5^\circ.6$, and 2004 VN₁₁₂–2013 RF₉₈ has $9^\circ.8$. In addition to this clustering, other obvious groupings are also visible. The dispersion of these additional groupings in ecliptic coordinates is similar to that of the set singled out by Brown & Batygin (2016), but their dispersion in q is considerably lower. ETNOs (82158) 2001 FP₁₈₅, 2002 GB₃₂ and 2003 HB₅₇ have a nearly common line of apsides; the same can be said about (445473) 2010 VZ₉₈, 2007 VJ₃₀₅ and 2015 SO₂₀. The case for the first grouping is

¹ <http://ssd.jpl.nasa.gov/sbdb.cgi>

Table 2. Barycentric orbital elements and parameters — $q = a(1 - e)$, $Q = a(1 + e)$ is the aphelion distance, $\varpi = \Omega + \omega$, P is the orbital period, Ω^* and ω^* are Ω and ω in the interval $(-\pi, \pi)$ instead of the regular $(0, 2\pi)$ — of the known ETNOs. The statistical parameters are Q_1 , first quartile, Q_3 , third quartile, IQR, interquartile range, OL, lower outlier limit ($Q_1 - 1.5\text{IQR}$), and OU, upper outlier limit ($Q_3 + 1.5\text{IQR}$). Input data as in Table 1.

Object	a (au)	e	i ($^\circ$)	Ω ($^\circ$)	ω ($^\circ$)	ϖ ($^\circ$)	q (au)	Q (au)	P (yr)	Ω^* ($^\circ$)	ω^* ($^\circ$)
82158	215.97915	0.84141	30.80134	179.35892	6.88451	186.24343	34.25244	397.70586	3172.01164	179.35892	6.88451
Sedna	506.08846	0.84945	11.92856	144.40251	311.28569	95.68820	76.19098	935.98594	11377.75735	144.40251	-48.71431
148209	221.97188	0.80122	22.75598	128.28590	316.68922	84.97512	44.12267	399.82108	3304.94285	128.28590	-43.31078
445473	153.36100	0.77602	4.51050	117.39858	313.72557	71.12415	34.35048	272.37152	1897.97030	117.39858	-46.27443
2002 GB ₃₂	206.50931	0.82887	14.19246	177.04395	37.04720	214.09115	35.33979	377.67883	2965.69498	177.04395	37.04720
2003 HB ₅₇	159.66557	0.76138	15.50028	197.87107	10.82977	208.70084	38.09895	281.23218	2016.20147	-162.12893	10.82977
2003 SS ₄₂₂	197.89567	0.80078	16.78597	151.04690	209.92864	0.97554	39.42455	356.36679	2782.09180	151.04690	-150.07136
2004 VN ₁₁₂	327.43521	0.85548	25.54761	66.02280	326.99699	33.01979	47.32201	607.54841	5921.13675	66.02280	-33.00301
2005 RH ₅₂	153.67748	0.74624	20.44577	306.11067	32.53853	338.64920	38.99710	268.35786	1903.84838	-53.88933	32.53853
2007 TG ₄₂₂	502.04248	0.92916	18.59530	112.91071	285.68512	38.59583	35.56265	968.52230	11241.58933	112.91071	-74.31488
2007 VJ ₃₀₅	192.09934	0.81684	11.98376	24.38239	338.33491	2.71730	35.18470	349.01398	2660.76077	24.38239	-21.66509
2010 GB ₁₇₄	351.12735	0.86169	21.56245	130.71444	347.24510	117.95954	48.56288	653.69182	6575.27641	130.71444	-12.75490
2012 VP ₁₁₃	263.16564	0.69436	24.05155	90.80392	293.54965	24.35357	80.43515	445.89613	4266.39240	90.80392	-66.45035
2013 GP ₁₃₆	149.78673	0.72587	33.53904	210.72729	42.47818	253.20547	41.06079	258.51267	1832.00656	-149.27271	42.47818
2013 RF ₉₈	317.06525	0.88557	29.60066	67.53381	316.37528	23.90909	36.28242	597.84808	5642.08982	67.53381	-43.62472
2015 SO ₂₀	164.90289	0.79885	23.41106	33.63383	354.83023	28.46406	33.17008	296.63570	2116.21317	33.63383	-5.16977
Mean	255.17334	0.81082	20.32577	133.64048	221.52654	107.66702	43.64735	466.69932	4354.74900	66.14048	-25.97346
Std. dev.	116.48633	0.06105	7.72495	71.95062	140.15770	102.40843	14.31074	226.78010	3103.33812	105.71229	49.06288
Median	211.24423	0.80903	21.00411	129.50017	302.41767	78.04963	38.54802	387.69235	3068.85331	101.85731	-27.33405
Q_1	163.59356	0.77236	15.17332	84.98639	41.12044	27.43644	35.30102	292.78482	2091.21024	31.32097	-46.88440
Q_3	319.65774	0.85096	24.42556	177.62269	319.26616	191.85778	44.92251	600.27317	5711.85155	134.13646	7.87082
IQR	156.06418	0.07860	9.25224	92.63630	278.14573	164.42135	9.62149	307.48835	3620.64131	102.81549	54.75523
OL	-70.50272	0.65446	1.29496	-53.96806	-376.09815	-219.19558	20.86879	-168.44770	-3339.75172	-122.90226	-129.01724
OU	553.75402	0.96886	38.30393	316.57714	736.48475	438.48980	59.35474	1061.50568	11142.81351	288.35969	90.00366
Statistics of Sedna, 148209, 2004 VN ₁₁₂ , 2007 TG ₄₂₂ , 2010 GB ₁₇₄ , 2012 VP ₁₁₃ and 2013 RF ₉₈											
Mean	355.55661	0.83956	22.00602	105.81058	313.97529	59.78588	52.63982	658.47340	6904.16927	105.81058	-46.02471
Std. dev.	110.14455	0.07477	5.60287	31.46021	20.47089	38.76357	18.27509	220.42583	3199.11104	31.46021	20.47089
Median	327.43521	0.85548	22.75598	112.91071	316.37528	38.59583	47.32201	607.54841	5921.13675	112.91071	-43.62472
Q_1	290.11545	0.82534	20.07888	79.16886	302.41767	28.68668	40.20255	521.87211	4954.24111	79.16886	-57.58233
Q_3	426.58491	0.87363	24.79958	129.50017	321.84310	90.33166	62.37693	794.83888	8908.43287	129.50017	-38.15690
IQR	136.46947	0.04829	4.72070	50.33131	19.42543	61.64498	22.17438	272.96677	3954.19176	50.33131	19.42543
OL	85.41124	0.75290	12.99782	3.67190	273.27952	-63.78080	6.94097	112.42195	-977.04653	3.67190	-86.72048
OU	631.28912	0.94607	31.88063	204.99713	350.98125	182.79914	95.63851	1204.28903	14839.72051	204.99713	-9.01875

particularly strong. Out of 16 known ETNOs, only five reach pericentre north from the ecliptic, i.e. $B_q > 0^\circ$; these objects are 82158, 2002 GB₃₂, 2003 HB₅₇, 2005 RH₅₂ and 2013 GP₁₃₆. This represents a 2σ departure from an isotropic distribution in B_q , where $\sigma = \sqrt{n}/2$ is the standard deviation for binomial statistics. This marginally significant result suggests that an unknown massive perturber has aligned the apsidal orientation of these objects, but the Planet Nine hypothesis cannot explain this pattern (Batygin & Brown 2016); another perturber is needed as the line of apsides is scarcely affected by indirect perturbations from the known planets. A nearly common line of apsides is also expected in a set of objects resulting from the break-up of a single object at pericentre. Such scenario might be linked to some of the groupings observed.

In Table 1 we show the current values of the position in the sky of the poles of the orbits of the known ETNOs computed using the data in Table 2; the ecliptic coordinates of the pole are $(L_p, B_p) = (\Omega - 90^\circ, 90^\circ - i)$. Fig. 2 shows the poles of the known ETNOs and also those of the known planets of the Solar system and various nominal orbits of Planet Nine (epoch 2457600.5 JD). The

objects singled out in Brown & Batygin (2016) and Planet Nine appear to exhibit a relative arrangement in terms of position of their orbital poles similar to the one existing between Neptune and Pluto. For this group, the average polar separation is $16^\circ \pm 8^\circ$, but the pair 148209–2010 GB₁₇₄ has $1^\circ 5'$, 2004 VN₁₁₂–2013 RF₉₈ has $4^\circ 1'$, 148209–2007 TG₄₂₂ has $6^\circ 8'$, 2007 TG₄₂₂–2010 GB₁₇₄ has $6^\circ 8'$, and 2007 TG₄₂₂–2012 VP₁₁₃ has $9^\circ 6'$. On the other hand, the ETNOs 2002 GB₃₂ and 2003 HB₅₇ not only exhibit apsidal alignment but their orbital poles are also very close.

As for the overall clustering in orbital parameter space, it has been claimed that the ETNOs exhibit clustering in the values of their ω (Trujillo & Sheppard 2014), e and i (de la Fuente Marcos & de la Fuente Marcos 2014), and Ω (Brown & Firth 2016). Table 2 presents the descriptive statistics of the known ETNOs; in this table, unphysical values are shown for completeness. The bottom block of statistics in Table 2 (see also Appendix A) focuses on the seven ETNOs singled out in Brown & Batygin (2016). The overall statistics is only slightly different from that of the heliocentric orbital elements. The mean value of the barycentric e of the known

ETNOs amounts to 0.81 ± 0.06 , the barycentric i is $20^\circ \pm 8^\circ$, the barycentric Ω is $134^\circ \pm 72^\circ$, and the barycentric ω is $-26^\circ \pm 49^\circ$ (see ω^* in Table 2). Clustering in e may be due to selection effects, but the others cannot be explained as resulting from observational biases, they must have a dynamical origin (de la Fuente Marcos & de la Fuente Marcos 2014). For the ETNO sample in Brown & Batygin (2016), the average values of the barycentric orbital parameters are $e = 0.84 \pm 0.07$, $i = 22^\circ \pm 6^\circ$, $\Omega = 106^\circ \pm 31^\circ$ and $\omega = 314^\circ \pm 20^\circ$.

Regarding the issue of statistical outliers and assuming that outliers are observations that fall below $Q_1 - 1.5$ IQR or above $Q_3 + 1.5$ IQR, where Q_1 is the first quartile, Q_3 is the third quartile, and IQR is the interquartile range, we observe a small but relevant number of outliers. For the entire sample, 2003 SS₄₂₂ is an outlier in terms of ω^* (see Table 2), Sedna and 2012 VP₁₁₃ are outliers in terms of q , and Sedna and 2007 TG₄₂₂ are outliers in terms of orbital period. In terms of size (not shown in the table), Sedna is a very significant outlier with $H = 1.6$ mag when the lower and upper limits for outliers are 4.7 mag and 8.7 mag, respectively. As for the sample of ETNOs in Brown & Batygin (2016), Sedna is a statistical outlier in terms of i .

3 VISIBILITY ANALYSIS

Here, we apply the Monte Carlo approach (Metropolis & Ulam 1949) described in de la Fuente Marcos & de la Fuente Marcos (2014) to construct visibility maps indicating the most probable location of this putative planet if it is near aphelion. Each Monte Carlo experiment consists of 10^7 test orbits uniformly distributed in parameter space. The analyses in e.g. Cowan et al. (2016), Fienga et al. (2016), Fortney et al. (2016), Ginzburg et al. (2016) and Linder & Mordasini (2016) strongly disfavour a present-day Planet Nine located at perihelion and they do not discard the aphelion which is also favoured in Brown & Batygin (2016).

3.1 Batygin & Brown (2016)

The resonant coupling mechanism described in Batygin & Brown (2016) emphasizes the existence of simultaneous apsidal anti-alignment and nodal alignment, i.e. $\Delta\varpi$ librates about 180° and $\Delta\Omega$ librates about 0° . The relative values of ϖ and Ω of the ETNO with respect to those of the perturber must oscillate in order to maintain orbital confinement but see Beust (2016) for a detailed analysis. In Batygin & Brown (2016), the value of ω of the putative Planet Nine is $138^\circ \pm 21^\circ$. It is also indicated that the average value of Ω for their six ETNOs is $113^\circ \pm 13^\circ$ and that of ω is $318^\circ \pm 8^\circ$. Applying the conditions for stability and using the other values discussed in their work, we generate a synthetic population of Planet Nines with $a \in (400, 1500)$ au, $e \in (0.5, 0.8)$, $i \in (15, 45)^\circ$, $\Omega \in (100, 126)^\circ$ and $\omega \in (117, 159)^\circ$. Fig. 3, left-hand panels, shows the distribution in equatorial coordinates of the set of studied orbits. In this figure, the value of the parameter in the appropriate units is colour coded following the scale printed on the associated colour box. The location of the Galactic disc appears in panel D (inclination). The background stellar density is the highest towards this region. The distribution of Q , a and e is rather uniform as expected because the location in the sky of Planet Nine does not depend on these parameters (see above). The distribution in declination depends on i and ω ; those orbits with higher values of i reach aphelion at lower declinations, the same behaviour is observed for the ones with lower values of ω . The location in right ascension mainly depends on the value of Ω , both increasing in direct proportion. Fig. 4, left-hand

panels, shows that the frequency distribution in right ascension and declination is far from uniform; the probability of finding an orbit reaching aphelion is highest in the region limited by $\alpha \in (4.5, 5.5)^h$ and $\delta \in (6, 9)^\circ$. However, the mean values of Ω and ω for the six ETNOs of interest differ from those in Table A1.

3.2 Brown & Batygin (2016)

The Planet Nine hypothesis has been further developed in Brown & Batygin (2016). In this new work, the volume of orbital parameter space linked to the putative planet for an assumed mass of $10 M_\oplus$ is enclosed by $a \in (500, 800)$ au, $e \in (0.32, 0.74)$, $i \in (22, 40)^\circ$, $\Omega \in (72.2, 121.2)^\circ$ and $\omega \in (120, 160)^\circ$. Figs 3 and 4, second to left-hand panels, show similar trends to the previous ones but now the distribution in equatorial coordinates of the aphelia is wider. The probability is highest in the region limited by $\alpha \in (3, 5)^h$ and $\delta \in (-1, 10)^\circ$. This enlarges the optimal search area significantly. However, they use a value of l_q of $241^\circ \pm 15^\circ$ that is based on a value of 61° for the seven ETNOs so Δl_q —not $\Delta\varpi$ — librates about 180° ; the average value of l_q for these ETNOs from Table 1 is $62^\circ \pm 38^\circ$, the average value of ϖ is $60^\circ \pm 39^\circ$.

3.3 Enforcing apsidal anti-alignment

Here, we enforce apsidal anti-alignment and nodal alignment, using the data in Table 2, bottom section, and considering the Planet Nine orbital parameter domain defined by $a \in (600, 800)$ au, $e \in (0.5, 0.7)$, $i \in (22, 40)^\circ$, $\Omega \in (74.4, 137.3)^\circ$ and $\omega \in (113.5, 154.4)^\circ$. Figs 3 and 4, second to right-hand panels, show that in this scenario, Planet Nine is most likely to be moving within $\alpha \in (3.0, 5.5)^h$ and $\delta \in (-1, 6)^\circ$, if it is near aphelion. If the data in Table A1 are used instead, then $\Omega \in (87, 117)^\circ$ and $\omega \in (118.5, 148.8)^\circ$ and we obtain Figs 3 and 4, right-hand panels. In this case, the putative planet is most likely moving within $\alpha \in (3.5, 4.5)^h$ and $\delta \in (-1, 2)^\circ$, i.e. projected towards the separation between the constellations of Taurus and Eridanus. In terms of probability, now the most likely location of Planet Nine is at $\alpha \sim 4^h$ and $\delta \sim 0:5$, in Taurus. This area is compatible with Orbit A in de la Fuente Marcos et al. (2016).

4 CONCLUSIONS

In this paper, we have re-analysed the various clusterings in ETNO orbital parameter space claimed in the literature and explored the visibility of Planet Nine within the context of improved constraints. Our results confirm the findings in Batygin & Brown (2016) and Brown & Batygin (2016) regarding clustering but using barycentric orbits. However, the observed overall level of clustering may not be maintained by a putative Planet Nine alone, other perturbers should exist. Summarizing:

- We confirm the existence of apsidal alignment and similar projected pole orientations among the currently known ETNOs. These patterns are consistent with the presence of perturbers beyond Pluto and/or, less likely, break-up of large asteroids at perihelion.
- If Planet Nine is at aphelion, it is most likely moving within $\alpha \in (3.0, 5.5)^h$ and $\delta \in (-1, 6)^\circ$ if $\Delta\varpi \sim 180^\circ$ and $\Delta\Omega \sim 0^\circ$.

ACKNOWLEDGEMENTS

We thank two anonymous referees for their constructive reports, and S. J. Aarseth, D. P. Whitmire, G. Carraro, D. Fabrycky, A. V.

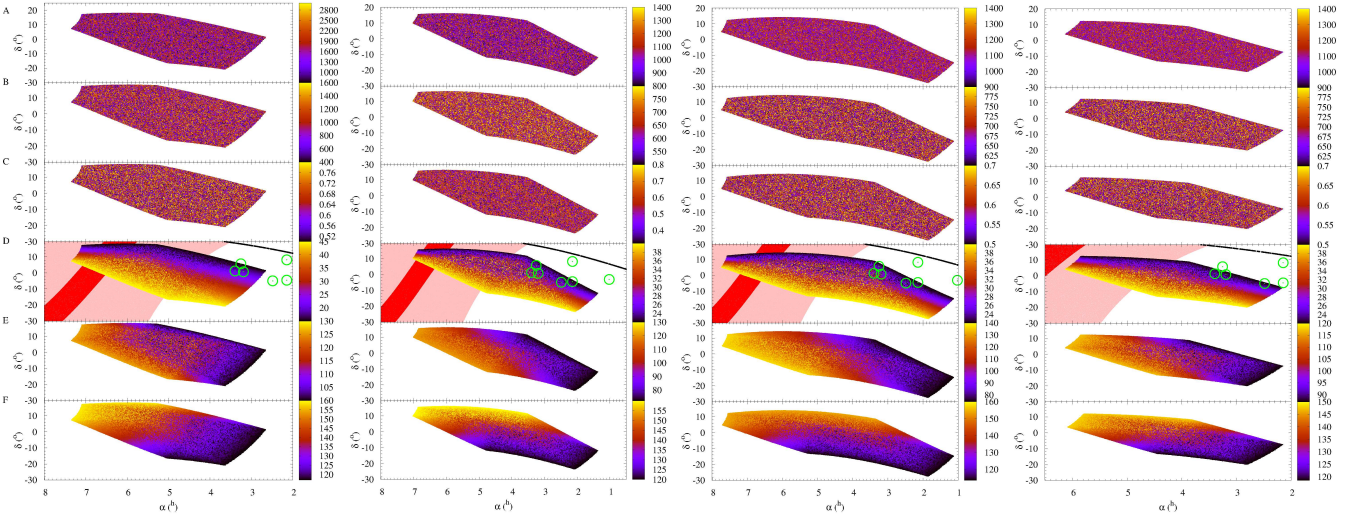


Figure 3. Distribution in equatorial coordinates of the aphelia of the studied orbits as a function of various orbital parameters: Q (panel A), a (panel B), e (panel C), i (panel D), Ω (panel E), and ω (panel F). The left-hand panels show results using the sets of orbits in Batygin & Brown (2016), those of orbits from Brown & Batygin (2016) are displayed in the second to left-hand panels; the second to right-hand panels and the right-hand panels focus on the set of orbits described in Sect. 3.3, imposing $\Delta\varpi \sim 180^\circ$ and $\Delta\Omega \sim 0^\circ$ using the data in Table 2 and A1, respectively. In panel D, the green circles give the location at discovery of known ETNOs (see table 2 in de la Fuente Marcos & de la Fuente Marcos 2016a), in red we have the Galactic disc that is arbitrarily defined as the region confined between galactic latitude -5° and 5° , in pink the region enclosed between galactic latitude -30° and 30° , and in black the ecliptic.

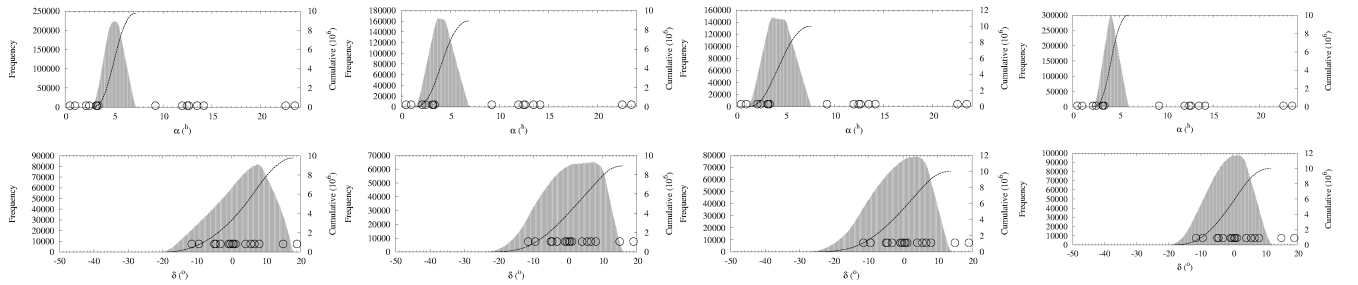


Figure 4. Frequency distribution in equatorial coordinates (right ascension, top panel, and declination, bottom panel) of the virtual orbits in Fig. 3. The number of bins is $2n^{1/3}$, where n is the number of virtual orbits plotted, error bars are too small to be seen. The black circles correspond to data in table 2 of de la Fuente Marcos & de la Fuente Marcos (2016a).

Tutukov, S. Mashchenko, S. Deen and J. Higley for comments on ETNOs and trans-Plutonian planets. This work was partially supported by the Spanish ‘Comunidad de Madrid’ under grant CAM S2009/ESP-1496. In preparation of this paper, we made use of the NASA Astrophysics Data System, the ASTRO-PH e-print server and the MPC data server.

REFERENCES

Batygin K., Brown M. E., 2016, *AJ*, 151, 22
 Beust H., 2016, *A&A*, 590, L2
 Brasser R., Schwamb M. E., 2015, *MNRAS*, 446, 3788
 Bromley B. C., Kenyon S. J., 2016, *ApJ*, 826, 64
 Brown M. E., Batygin K., 2016, *ApJ*, 824, L23
 Brown R. B., Firth J. A., 2016, *MNRAS*, 456, 1587
 Cowan N. B., Holder G., Kaib N. A., 2016, *ApJ*, 822, L2
 de la Fuente Marcos C., de la Fuente Marcos R., 2014, *MNRAS*, 443, L59
 de la Fuente Marcos C., de la Fuente Marcos R., 2016a, *MNRAS*, 459, L66
 de la Fuente Marcos C., de la Fuente Marcos R., 2016b, *MNRAS*, 460, L64
 de la Fuente Marcos C., de la Fuente Marcos R., Aarseth S. J., 2015, *MNRAS*, 446, 1867

de la Fuente Marcos C., de la Fuente Marcos R., Aarseth S. J., 2016, *MNRAS*, 460, L123
 Feng F., Bailer-Jones C. A. L., 2015, *MNRAS*, 454, 3267
 Fienga A., Laskar J., Manche H., Gastineau M., 2016, *A&A*, 587, L8
 Fortney J. J. et al., 2016, *ApJ*, 824, L25
 Ginzburg S., Sari R., Loeb A., 2016, *ApJ*, 822, L11
 Giorgini J. D. et al., 1996, *BAAS*, 28, 1158
 Gomes R. S., Soares J. S., Brasser R., 2015, *Icarus*, 258, 37
 Jílková L., Portegies Zwart S., Pijloo T., Hammer M., 2015, *MNRAS*, 453, 3157
 Kenyon S. J., Bromley B. C., 2015, *ApJ*, 806, 42
 Kenyon S. J., Bromley B. C., 2016, *ApJ*, 825, 33
 Li G., Adams F. C., 2016, *ApJ*, 823, L3
 Linder E. F., Mordasini C., 2016, *A&A*, 589, A134
 Luhman K. L., 2014, *ApJ*, 781, 4
 Madigan A.-M., McCourt M., 2016, *MNRAS*, 457, L89
 Malhotra R., Volk K., Wang X., 2016, *ApJ*, 824, L22
 Metropolis N., Ulam S., 1949, *J. Am. Stat. Assoc.*, 44, 335
 Murray C. D., Dermott S. F., 1999, *Solar System Dynamics*. Cambridge Univ. Press, Cambridge, p. 97
 Mustill A. J., Raymond S. N., Davies M. B., 2016, *MNRAS*, 460, L109
 Pauč R., Klačka J., 2016, *A&A*, 589, A63
 Trujillo C. A., Sheppard S. S., 2014, *Nature*, 507, 471

APPENDIX A: FURTHER DETAILS ON THE COMPARISON WITH THE RESULTS OF BROWN & BATYGIN (2016)

According to the heliocentric orbital solutions publicly available from the SBDB, the six (not seven) objects singled out in Batygin & Brown (2016) all have values of the heliocentric semimajor axis, a , larger than 257 au; Brown & Batygin (2016) indicate that their semimajor axes are larger than 227 au. The six original objects in Batygin & Brown (2016)—namely, (90377) Sedna ($a = 499$ au), 2004 VN₁₁₂ ($a = 318$ au), 2007 TG₄₂₂ ($a = 483$ au), 2010 GB₁₇₄ ($a = 370$ au), 2012 VP₁₁₃ ($a = 258$ au) and 2013 RF₉₈ ($a = 307$ au)—do not have the largest values of the perihelion distance, only four of them—Sedna ($q = 76$ au), 2004 VN₁₁₂ ($q = 47$ au), 2010 GB₁₇₄ ($q = 49$ au) and 2012 VP₁₁₃ ($q = 80$ au)—are in this situation. In Brown & Batygin (2016), it is said that the seven objects with $a > 227$ au are singled out. However, fig. 1(a) in Brown & Batygin (2016) highlights in red only six objects (those singled out in Batygin & Brown 2016), not seven; (148209) 2000 CR₁₀₅ ($a = 226$ au, $q = 44$ au), which has the eighth largest value of the heliocentric semimajor axis and the fifth largest perihelion distance, appears in green in that figure. The ETNO with the seventh largest value of the heliocentric semimajor axis is (82158) 2001 FP₁₈₅ ($a = 227$ au, $q = 34$ au), not 148209 as erroneously stated in Brown & Batygin (2016). Our analysis in Figs 1 and 2 shows that 82158 is unlikely to be dynamically connected with the original six ETNOs singled out in Batygin & Brown (2016), but 148209 very probably is. Therefore, the seven objects of interest within the context of the Planet Nine hypothesis are: Sedna, 148209, 2004 VN₁₁₂, 2007 TG₄₂₂, 2010 GB₁₇₄, 2012 VP₁₁₃ and 2013 RF₉₈.

In terms of barycentric (not heliocentric) orbits, see Table 2, 148209 has the seventh largest value of the semimajor axis and 82158 has the eighth largest.

Table A1 shows the statistics for the six original objects in Batygin & Brown (2016); the average values of the orbital parameters are $e = 0.85 \pm 0.08$, $i = 22^\circ \pm 6^\circ$, $\Omega = 102^\circ \pm 33^\circ$ and $\omega = 314^\circ \pm 22^\circ$ (these values have been used in the discussion in Section 3.1). The average angular separation at pericentre for this group is $45^\circ \pm 34^\circ$ and the average polar separation is $16^\circ \pm 8^\circ$. For the sample of ETNOs in Batygin & Brown (2016), both 2007 TG₄₂₂ and 2012 VP₁₁₃ are statistical outliers in terms of e (see Tables 2 and A1).

The expression for the eccentricity of the putative Planet Nine in Brown & Batygin (2016) produces negative values for masses under $\sim 6.38 M_\oplus$ and the lower limit of the value of the semimajor axis. Production of unphysical values is the main reason why it has not been applied to select the range in eccentricities used in Section 3.3.

This paper has been typeset from a $\text{\TeX}/\text{\LaTeX}$ file prepared by the author.

Table A1. As Table 2, bottom section, but only for the six objects singled out in Batygin & Brown (2016): (90377) Sedna, 2004 VN₁₁₂, 2007 TG₄₂₂, 2010 GB₁₇₄, 2012 VP₁₁₃ and 2013 RF₉₈. Source data in Table 2, top section.

Parameter	a (au)	e	i (°)	Ω (°)	ω (°)	ϖ (°)	q (au)	Q (au)	P (yr)	Ω^* (°)	ω^* (°)
Mean	377.82073	0.84595	21.88102	102.06470	313.52297	55.58767	54.05935	701.58211	7504.04034	102.06470	-46.47703
Std. dev.	101.95284	0.07978	6.12694	32.70823	22.38639	40.68277	19.59205	206.62725	3042.77393	32.70823	22.38639
Median	339.28128	0.85859	22.80700	101.85731	313.83049	35.80781	47.94245	630.62012	6248.20658	101.85731	-46.16951
Q ₁	319.65774	0.85096	19.33709	73.35133	297.98366	26.52012	39.04232	600.27317	5711.85155	73.35133	-62.01634
Q ₃	464.31370	0.87960	25.17359	126.26351	324.34156	81.41511	69.28395	865.41241	10075.01110	126.26351	-35.65844
IQR	144.65595	0.02864	5.83650	52.91217	26.35790	54.89498	30.24163	265.13924	4363.15955	52.91217	26.35790
OL	102.67381	0.80799	10.58233	-6.01693	258.44681	-55.82235	-6.32013	202.56430	-832.88777	-6.01693	-101.55319
OU	681.29763	0.92256	33.92835	205.63177	363.87841	163.75758	114.64641	1263.12127	16619.75042	205.63177	3.87841